EFFICACY OF HOST-KINASE INHIBITORS AS ANTIVIRAL AGENTS AGAINST VENEZUELAN EQUINE ENCEPHALITIS VIRUS

by

Tyler Lark

A Thesis
Submitted to the
Graduate Faculty
of
George Mason University
in Partial Fulfillment of
The Requirements for the Degree
of
Master of Science
Biology

Committee:

_____	Dr. Aarthi Narayanan, Thesis Director
_____	Dr. Kylene Kehn-Hall, Committee Member
_____	Dr. Ancha Baranova, Committee Member
_____	Dr. Iosif Vaisman, Director, School of Systems Biology
_____	Dr. Donna M. Fox, Associate Dean, Office of Student Affairs & Special Programs, College of Science
_____	Dr. Peggy Agouris, Dean, College of Science
Date: _____	Fall Semester 2017 George Mason University Fairfax, VA

Efficacy of Host-Kinase Inhibitors as Antiviral Agents Against Venezuelan Equine Encephalitis Virus

A thesis submitted in partial fulfillment of the requirements for the degree of Master of Science at George Mason University

By

Tyler Lark
Bachelor of Science
Lycoming College, 2010

Director: Aarthi Narayanan, Assistant Professor
Department of Biology

Fall Semester, 2017
George Mason University
Fairfax, VA

DEDICATION

This is dedicated to my loving wife Madina, without whom I would not have been able to make it this far, and my son Dean and dog Moose, all who have inspired me to further my education.

ACKNOWLEDGEMENTS

I would like to thank my family for their support and motivation. I would like to thank Dr. Aarthi Narayanan for her guidance and mentorship over these past few years. I would like to thank my committee members Dr. Kehn-Hall and Dr. Baranova their time and help. I would also like to thank all the lab members I've worked with over the years.

TABLE OF CONTENTS

LIST OF FIGURES

Figure Page

LIST OF ABBREVIATIONS

Abbreviations

AP2 Associated Protein Kinase 1……AAK1

Azaindole……Aza

Clathrin Assoociated Adaptor Protein 1/2 ……AP1/AP2

Cycling G-Associated Kinase……GAK

Cytotoxic Concentration……CC_{50}

Dengue Virus……DENV

Eastern Equine Encephalitis Virus……EEEV

Ebola Virus……EBOV

Effective Concentration……EC_{50}

Erlotinib……Erl

Hepatitis C Virus……HCV

Selective Index……SI

Venezuelan Equine Encephalitis Virus……..VEEV

Western Equine Encephalitis Virus……WEEV

ABSTRACT

EFFICACY OF HOST-KINASE INHIBITORS AS ANTIVIRAL AGENTS AGAINST VENEZUELAN EQUINE ENCEPHALITIS VIRUS

Tyler Lark, M.S.

George Mason University, 2017

Thesis Director: Dr. Aarthi Narayanan

Venezuelan equine encephalitis virus (VEEV) is a New World alphavirus that is naturally transmitted through mosquito vectors resulting in human infections. This virus is classified as a category B pathogen and a select agent as it is highly infectious and retains infectivity when transmitted as an aerosol. There is currently no therapeutic or vaccine candidate that is available to the civilian population for the treatment of VEEV exposures. With the ability of viruses to develop resistance to antiviral strategies that target viral components, it will be of strategic value to target specific host proteins to inhibit the viral life-cycle. Such host-based therapeutic candidates are also likely to find broad spectrum applicability in the treatment of infections by of other viral pathogens in addition to VEEV that employ the same host-based candidates. We show that inhibition of host kinases, AP2-associated protein kinase 1 (AAK1) and cyclin G-associated kinase (GAK), associated with clathrin-mediated endocytosis and intracellular trafficking results in a decrease of VEEV load in

infected cells. siRNA knockdown of AAK and GAK yielded a decrease in viral titers along with alteration of viral protein levels. The small molecules azaindole and erlotinib (FDA approved) were found to have strong antiviral properties. Both drugs affected the ability of the virion to traffic effectively through the cell, preventing the movement from the plasma membrane and potentially, the ER network. Time of addition experiments showed that the drugs exhibit therapeutic potential, as both worked against established infections. These results show the effectiveness of AAK and GAK inhibitors in inhibiting VEEV infection. Ongoing research is exploring the mechanisms involved in this inhibitory process.

CHAPTER 1: INTRODUCTION

VEEV is a member of the *Togaviridae* family of viruses, which is composed of the genera Alphavirus and Rubivirus. The alphaviruses are subdivided into two categories: Old World and New World alphaviruses. Old World alphaviruses consist of Semliki Forest virus, chikungunya virus, and Sindbis virus while New World alphaviruses include VEEV, eastern equine encephalitis virus (EEEV), and western equine encephalitis virus (WEEV). The two subsets of alphaviruses differ in terms of their geographic distribution and associated symptoms. New World alphaviruses are found mainly in the Americas and can cause encephalitic outcomes in infections, while Old World alphaviruses are found mainly in Africa and Asia with arthritic symptoms being the most common result [1, 2].

VEEV maintains an enzootic life cycle using rodents as a reservoir and *Culex* sp. mosquitoes as a vector. It enters an epizootic life cycle when it is transmitted to equines or humans via the *Aedes* sp. of mosquitoes [3, 4]. There are six antigenic subtypes of VEEV (I-VI) and most are involved in the enzootic life cycle of the virus. The subtypes IAB and IC are the most common strains that are associated with epizootic outbreaks in equines and epidemics in humans [4, 5]. The first recognized outbreak of VEEV was in 1935 in Colombia and Venezuela, with numerous outbreaks occurring afterward in regions up to the southern portion of Texas, with some resulting in the infection of over 100,000 people

[5]. Spillover from the enzootic rodent life cycle has resulted in human outbreaks, and VEEV infected horses can distribute the virus through bodily fluids by means of direct contact or aerosols. Aside from infections through infected organisms, there are also numerous reports of infections from aerosols in laboratory settings [3]. The ability of the virus to readily replicate to high titers and retain infectivity as aerosol has given VEEV the ability to be an effective biological weapon [3-5]. There are currently no effective vaccines for VEEV that are offered to the general public. TC-83 is an attenuated strain that is offered as a live-attenuated vaccine for at risk personnel. In humans, while there is a strong seroconversion, there is a high rate of side effects, which include fever, nausea, malaise, myalgia, and headaches. C-84, a formalin inactivated form of TC-83, is provided only under conditions when TC-83 did not result in robust seroconversion and a booster shot is necessary. C-84 by itself, is not a robust inducer of protective immunity as compared to TC-83 [6]. There are also no effective, FDA approved treatment strategies to treat exposure to VEEV.

VEEV is a spherical and enveloped virus, with a diameter of 70nm and icosahedral symmetry of T=4. The virion contains a ~11.4kb positive sense, single stranded RNA genome, which contains a 5` cap and 3` poly(A) tail (Figure 1). The 5` end of the genome encodes for 4 nonstructural proteins (nsP1-4) while the 3` end produces 5 structural proteins (capsid, E1-E3, 6K) [7-10]. The structural proteins are responsible for the entry into the host cell and virion assembly for exiting. Capsid binds viral RNA and stimulates nucleocapsid assembly, as well as inhibits the import of cellular proteins into the nuclues. E2 binds to the host receptor and E1 mediates membrane fusion, E3 activates E1, and 6K

forms ion channels within the host cell and aids in the trafficking of the immature E1 and E2 proteins. The nonstructural proteins' main functions are associated with viral replication. nsP1 is a membrane anchored protein that is responsible for the synthesis and capping of RNA; nsP2 acts as a RNA helicase and a protease, cleaving the nonstructural polyprotein into its individual elements; nsP3 is required for minus-strand and subgenomic RNA synthesis; nsP4 acts as an RNA polymerase [1, 11-12].

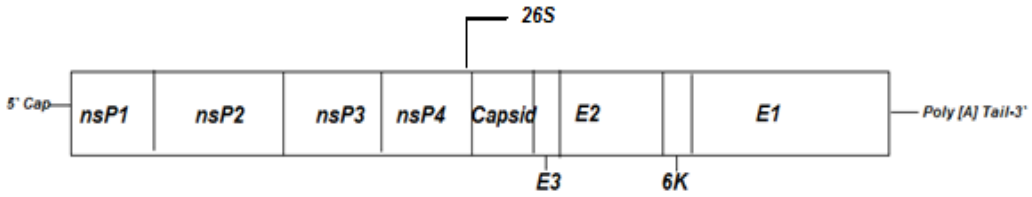

Figure 1. A schematic representation of the VEEV genome. The VEEV positive ssRNA genome is ~11.5kb in length and contains a 5`cap and poly[A] tail. It codes for four nonstructural proteins and 5 structural proteins.

With the need for more effective therapeutic candidates against VEEV, it is a promising avenue to look at host proteins that interact with the virus to inhibit critical events that are required for the establishment and maintenance of VEEV infection. By targeting host proteins, there is less concern of viral mutations that can lead to the development of viral resistance. Inhibition of host proteins would also have the potential

for combating other viruses (broad spectrum inhibition) including Old World and other New World alphaviruses.

Host-based enzymatic machinery constitutes an attractive spectrum of targets that may be used for development of therapeutics against VEEV. Our laboratory has demonstrated that host-derived kinases including IKKβ and MEK/ERK are required for the maintenance of VEEV infection and their requirement extends to EEEV and WEEV. The IKK complex is a kinase of the NFκB pathway, which is activated by VEEV as evidenced by phosphorylation in infected cells and an increase in viral production in IKKβ overexpression cells. Treatment with known inhibitors of IKKβ, BAY-11-7082, BAY-11-7085, and IKK2-IV, lead to a decrease in viral production [8]. ERK is a MAPK protein that responds to stress stimuli, such as viral infections, and leads to the downstream events of inflammation and cell death. Experimental data suggested that VEEV infections, as well as EEEV and WEEV, may result in the phosphorylation of multiple viral proteins within the ERK signaling cascade. Treatment of infected cells with Ag-126, an inhibitor of ERK, lead to a decrease in viral production [13]. Thus, host-based kinases have the potential to constitute broad spectrum targets for the development of inhibitors against alphaviruses.

VEEV, as most enveloped viruses, enters the host cell through the binding to cell surface receptors, such as the laminin binding protein [14] and being endocytosed via clathrin mediated pits [15, 16] (Figure 2). Clathrin is a trimeric protein that associates to form a lattice structure around endocytic vesicles from the plasma membrane and vesicles trafficking between the trans-Golgi network. Clathrin does not directly bind to the

membranes, but rather is connected via clathrin-associated adaptor proteins (APs) [17, 18]. These APs aid in the formation of the endosome, recruitment of the cargo, and the trafficking of the endosome and other vesicles, with AP1 being linked to the trans-Golgi network and AP2 to endocytosis at the plasma membrane [17, 19, 20]. Protein kinases play a crucial role in the functioning of these AP complexes. The serine/threonine kinases AP2-associated protein kinase 1 (AAK1) and cyclin G-associated kinase (GAK) are responsible for the activation of the APs. AAK1 binds to the α subunit of AP2 and phosphorylates the μ2 subunit at the T156 residue. This activation increases the affinity of AP2 for cargo sorting signals on the forming vesicle, increasing the uptake of the incoming cargo. AAK1 is expressed mainly at endocytic sites on the plasma membrane. GAK can also bind and phosphorylate AP2, as well as bind to the γ subunit of AP1 and phosphorylate the μ1 subunit at the T144 residue. GAK has similar functions as the kinase auxilin, however, auxilin is expressed only in neuronal cells whereas GAK is expressed ubiquitously. Unlike AAK1, GAK is expressed mainly in the cytosol and perinuclear region. GAK also functions in the recruitment of APs to the plasma membrane and intracellular organelles [21-23].

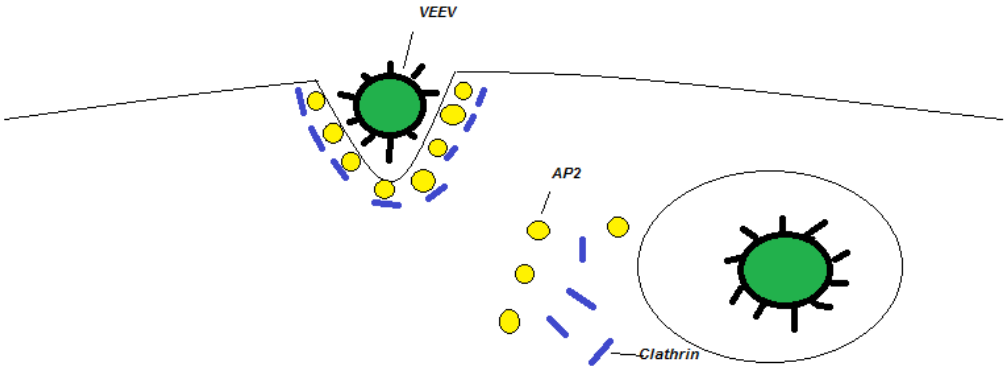

Figure 2. Viral entry utilizing clathrin-mediated endocytosis. After the binding of VEEV to a cell surface receptor, clathrin and adaptor proteins are recruited to the site. The adaptor proteins interact with the forming endosome and clathrin coats the vesicle to provide structure. After the endosome has matured and is en route to its destination, the clathrin and adaptor proteins dissociate and are recycled for further use.

AP1 and AP2 have been demonstrated to aid in the intracellular trafficking of several viruses. HCV, DENV and EBOV were shown to be dependent of AP1 and AP2 for effective growth. Along with this, inhibition of AAK1 and GAK in these studies was shown to decrease viral titers [24-26]. Such broad spectrum success with AAK1 and GAK inhibitors against multiple enveloped viruses suggested to us the possibility that New World alphaviruses may also be susceptible to inhibition by these inhibitors. As a first step, we found that a knockdown of kinases inhibits viral replication kinetics. Next, we examined the necessity of AAK1 and GAK for the establishment of a productive VEEV infection using small molecule inhibitors of AAK1 and GAK. We found that a knockdown of the kinases inhibits viral replication kinetics. The efficacy of two small molecule

candidates, one of which is FDA approved as an anti-cancer drug, that target AAK1 and GAK were tested against VEEV, with both exhibiting antagonistic effects on the ability of the virus to establish a productive infection. These data show the necessity of AAK1 and GAK for VEEV and we feel merits further investigation into the effects of targeting host proteins for managing viral infections.

CHAPTER 2: MATERIALS AND METHODS

Inhibitor Studies

U87MG cells were seeded into 96-well plates at a concentration of 10,000 cells per well and incubated at 37°C for 24 hours. The cells were pretreated with the inhibitors, Azaindole and Erlotinib, for 2 hours. The treatment media was removed and the viral infection proceeded for 1 hour at an MOI of 0.1. The viral media was removed and the treatment media was added back on. The plates were incubated at 37°C for 18 hours, followed by collection and storage of the supernatants at -80°C. For RT-qPCR studies, RNA was extracted using Qiagen RNA Extraction Kit according to the manufacturer's instructions.

Plaque Assays

Vero cells were seeded into 12-well plates at a concentration of $2.5x10^5$ cells per well and incubated at 37°C for 24 hours. Viral supernatant was diluted in DMEM by factors of 10 and added in duplicate to the wells. The plates were incubated for 1 hour, with occasional rocking, followed by the addition of 1mL of 1:1 EMEM:0.6% Agarose to each well. The plates were incubated at 37°C for 48 hours. A 10% formaldehyde solution was added to the wells and left at room temperature for ≥1 hour. A rinsing with diH_20 was used to

remove the agarose plugs. A 1% crystal violet stain was added and the plates were rocked for ~5 minutes. The plates were rinsed with diH_20 and plaques were counted and viral titers were determined (Average # Plaques/(Dilution Factor x Volume Virus added)) and recorded as PFU/mL.

Cell Viability Assays

U87MG cells were seeded into 96-white well plates at a concentration of 10,000 cells per well and incubated at 37°C for 24 hours. 200µL of media containing Aza (1-275µM), Erl (1-100µM), or siRNA (100nM) were added to each well and incubated at 37°C for 24 hours. The media was removed and 50µL CellTiter-Glo reagent and 50µL DMEM were added to the wells and shaken for 2 minutes. The plates were incubated at room temperature for 10 minutes and luminescence was detected using the DTX 880 multimode detector (Beckman Coulter).

Western Blot Analysis

Whole cell lysates were separated on a Tris-Glycine Gel and transferred to a polyvinyl difluoride membrane. The membranes were blocked with 1% milk in tris-buffered saline at room temperature. Primary antibodies to VEEV Capsid 1/1,000 (BEI: NR-9404) and Glycoprotein 1/1,000 (BEI: NR-9403), AAK1 1/1,000 (Invitrogen: PA5-20616), GAK 1/1,000 (Invitrogen: PA5-15321)and β-actin 1/1,000 (Abcam: ab49900) were added per the manufacturer's instructions. The blots with primary antibodies were incubated overnight at 4°C. Secondary antibodies (Goat anti-Rabbit, Goat anti-Mouse, Rabbit anti-Goat) were added (1/10,000) after two washes with TBS, followed by three additional

washes with TBS. Membranes were visualized using West Femto reagent and imaged using a ChemiDoc XRS system (Bio-Rad) and analyzed using Quantity One software (Bio-Rad).

siRNA Transfections

U87MG cells were seeded into a 12-well plate at a concentration of $7.5x10^4$ cells/well in serum free media and incubated for 24 hours at 37°C. AAK1 (GGUAUAUGUUGGAACCAGATT), GAK (CAGCAUCCAUAGGAAAAGATT), and a Silencer Select Negative Control No. 1 siRNA (Thermofisher: Catalog # 4390843) were diluted to a concentration of 100nM in serum free DMEM containing siRNA diluent and siIMPORTER reagent (MilliporeSigma: Catalog # 64-101), followed by incubation at room temperature for 5 minutes. The serum free media was removed from the wells and the wells were washed twice with pre-warmed serum free media. The siRNA containing media was added to the corresponding wells and incubated at 37°C for 4 hours. DMEM with serum was added to each well and incubated for 24 hours at 37°C. Infections proceeded as previously described.

RT-qPCR

Infections were setup as previously described. Intracellular RNA was extracted using Qiagen RNeasy Mini Kit (Catalog# 74106) and extracellular RNA was extracted using Qiagen QIAamp Viral RNA Mini Kit (Catalog# 52906), process was done following manufacturer's instructions. The PCR mixture was done using Quantitect One-step RT-PCR kit (Qiagen cat# 204443) and Verso 1-Step RT-qPCR Mix, ROX (ThermoFisher Cat#AB101A) according to manufacturer's instructions. Each amplification run contained

one negative control (blank reagent and water), and a series of Ribogreen measured TC83 RNA positive controls (10-fold serial dilutions of nucleic acid extracted from viral stocks). Used PrimeTime Assay XL Probe 5` 6-FAM/ZEN/3 IBFQ (IDT), primer 1 TCTGACAAGACGTTCCCAATCA (IDT) and primer 2 GAATAACTTCCCTCCGACCACA (IDT). The following thermal profile was used: single cycle 20 minutes at 50°C, 15 minutes at 95°C; 40 amplification cycles of 15 seconds at 95°C, 1 minute at 50°C. PCR was performed on ThermoFisher StepOnePlus Real-Time PCR System.

Immunofluorescence

For Azaindole studies, U87MG cells were pre-treated for 2 hours, infected at an MOI:1 for 1h, and fixed with 4% paraformaldehyde in PBS at 6hpi. For Erlotinib studies, U87MG cells were pre-treated for 2 hours, infected at an MOI:1 for 1h, and fixed with 4% paraformaldehyde at 10hpi. Cells were permeabilized with 0.1% Triton X-100 in PBS, incubated with primary antibodies specific to AP2 1/1,000, RCSA1 golgi marker 1/1000 (Cell Signaling: 12290), the calnexin ER marker 1/1000 (SC:11397), or VEEV GP 1/1,000, incubated with Alexa-Fluor secondary antibodies 1/500 (Alexa Flour 488 for green, 567 for red), and mounted with DAPI Fluoromount G. Images were taken using the 60X objective of a Nikon Eclipse TE2000 confocal microscope. All scale bars represent 20 microns.

CHAPTER 3: RESULTS

Knockdown of AAK1 and GAK Results in a Decrease in VEEV Load in Infected Cells

AAK1 and GAK are host kinases that have been shown to aid in the transport of various enveloped viruses from the cell membrane and at the trans-Golgi network to the cell membrane [24-26]. We hypothesized that these kinases will be essential for the establishment of a productive infection in VEEV infected cells. As a first step, we tested if depletion of endogenous AAK1 and GAK will influence VEEV replication. We also reasoned that siRNA based knockdown of the target genes will offer the most specific representation of the requirement of these two kinases for VEEV infection, as compared to small molecule inhibitors that may have additional off-target effects. We utilized the astroglioma cell line, U87MG for our studies as this cell line has been reported by our laboratory and peer laboratories as being able to support VEEV infection [8, 9]. U87MG cells were transfected with an siRNA targeting either AAK1, GAK, or a nonspecific negative control siRNA, with non-transfected mock cells maintained as a control. Cells were transfected with 100nM siRNA containing serum free media for 4 hours, followed by the addition of serum containing media and incubation for an additional 24 hours. Whole cell extracts were collected and analyzed via western blots for the expression of AAK1 and GAK protein levels, with protein levels being normalized to β-actin as a loading control.

The resulting data showed that there was a dramatic decrease in expression of both AAK1 (Figure 3A) and GAK (Figure 3B) in the siRNA transfected cells. Having shown that transfection with the siRNAs results in a decrease in protein expression, to assure that transfecting with the siRNAs does not result in cell death, we also verified if they are cytotoxic to U87MG cells. Cytotoxicity was determined using CellTiter-Glo, and results showed that depletion of AAK1 or GAK in the context of U87MG cells did not result in overt cytotoxicity (Figure 3C). Having shown that transfection with AAK1 and GAK siRNAs results in a decrease of the target proteins without showing cytotoxic effects on the cells, we next wanted to explore the effects of AAK1 and GAK depletion on VEEV infection. Cells were transfected as described earlier, infected with TC-83 at an MOI:0.1 for 1 hour, and incubated for 18 hours. Non-transfected cells were infected with TC-83 as a positive control and a transfection with nonspecific siRNA was used as a negative control. Intracellular vRNA was extracted and levels were measured via RT-qPCR. The resulting data showed a significant decrease in intracellular VEEV genomic copies for both AAK1 and GAK siRNA transfected cells compared to both controls (Figures 4A and 4B). Infectious viral titers (extracellular viral load) were measured by plaque assays. The infection was done as previously described, with the addition of cells being treated with a combination of AAK1 and GAK siRNA to determine the effect of a knockdown of both kinases on virus production. 10-fold serial dilutions of the viral supernatants were added to Vero cells, incubated for 48 hours and fixed and stained for plaque counting. When compared to the TC-83 and negative siRNA controls, there was a decrease of ~90% in infectious viral titers for AAK1, GAK, and AAK1/GAK treated cells. The combination of

AAK1 with GAK did not result in an additive effect in decreasing viral titers, with the levels produced being comparable to the individually treated cells (Figure 4C). Western blot analysis revealed a marked decrease in the presence of VEEV capsid protein along with a modest decrease in VEEV GP when AAK1 inhibited (Figure 4D), while inversely, there was a more robust decrease in GP than capsid when GAK is repressed (Figure 4E). This result may highlight the dependence each viral protein has on the respective kinases, with capsid being more reliant on AAK1 and the glycoprotein being dependent upon GAK for their processes in viral infection. Taken together, our experiments with siRNA mediated depletion of AAK1 and GAK revealed that these two kinases were important for the establishment of a productive VEEV infection.

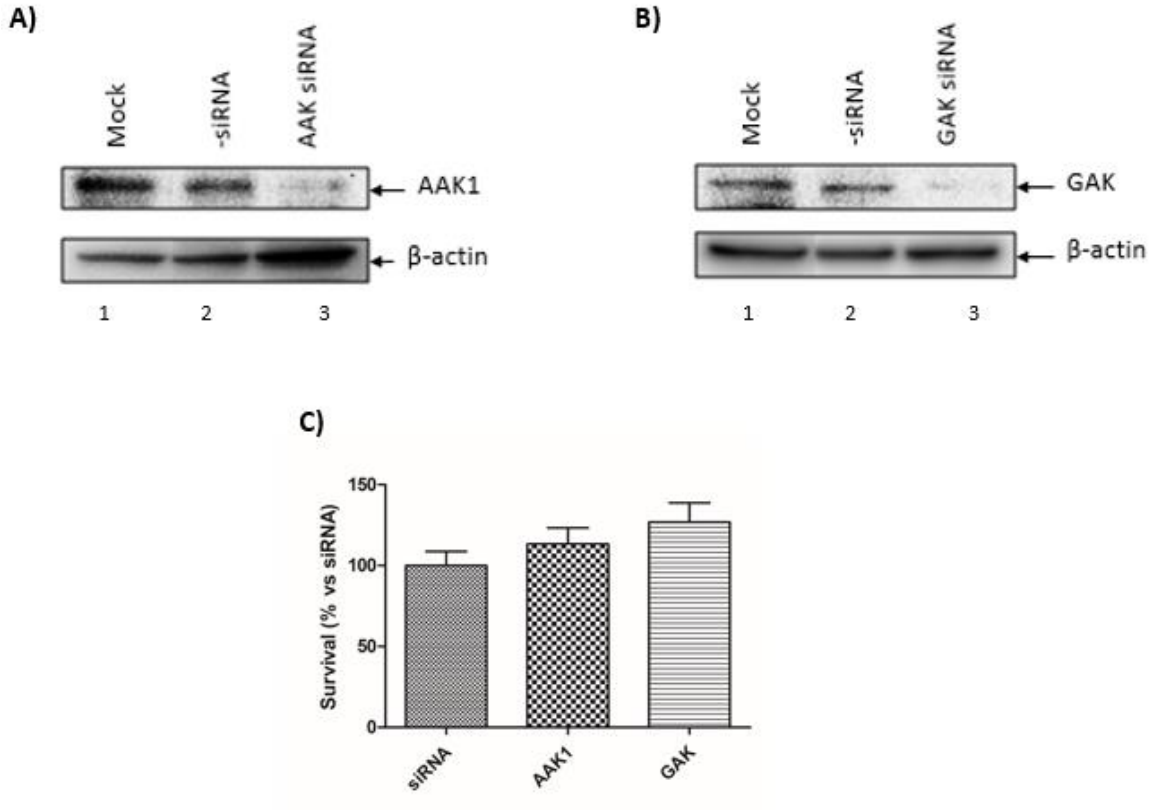

Figure 3. Transfection of U87MG cells with siRNA specific to AAK1/GAK results in a reduction of the host kinase being expressed. U87MG cells were transfected with 100nM AAK1, GAK, or a negative control siRNA using a siIMPORTER reagent in serum free DMEM. Whole cell extracts were collected for analysis at 10hpi. Whole cell extracts were lysed and run on a Tris-Glycine Gel for protein separation and transferred onto a polyvinyl difluoride membrane. Primary antibodies for AAK1 (A), GAK (B), and β-actin were added and imaged following secondary antibody addition. U87MG cells were transfected with AAK, GAK, or negative control siRNA for 24 hours and cell viability was quantified using CellTiter-Glo (C). A negative control siRNA and non-transfected mock were used for controls.

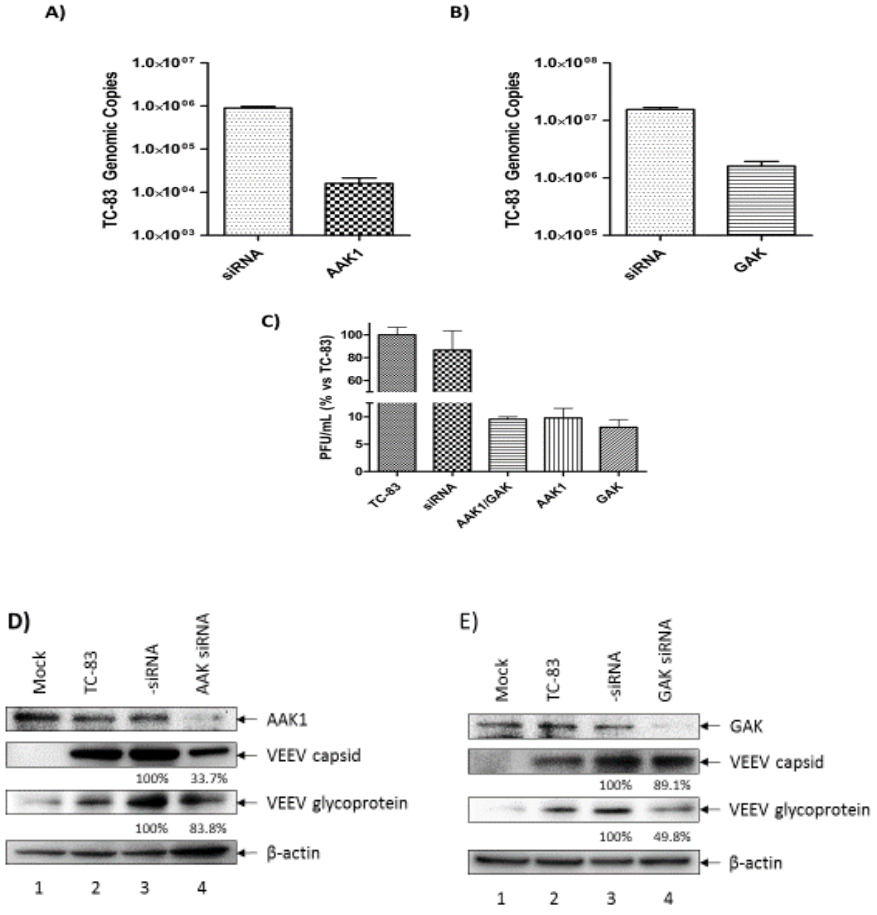

Figure 4. AAK1/GAK targeting siRNA inhibits VEEV protein production and life cycle. U87MG cells were transfected with 100nM AAK1, GAK, or a negative control siRNA using a siIMPORTER reagent in serum free DMEM. Cells were infected with TC-83 and supernatants and whole cell extracts were collected for analysis at 10hpi. Viral RNA was extracted and analyzed via RT-PCR for AAK1 (A) and GAK (B). Supernatants were diluted by factors of 10 and added to VERO cells for plaque forming capabilities (C). Whole cell extracts were lysed and run on a Tris-Glycine Gel for protein separation and transferred onto a polyvinyl difluoride membrane. Primary antibodies for AAK1 (D), GAK (E), VEEV capsid and glycoprotein, and β-actin were added and imaged following secondary antibody addition. Uninfected (Mock), TC-83, and a negative control siRNA were used for controls.

Treatment with Azaindole and Erlotinib Results in a Reduction in Viral Load

Azaindole (Aza) and Erlotinib (Erl) are known inhibitors of AAK1 and GAK [26, 27]. We wanted to test if the use of either inhibitor would have an antagonistic effect on TC-83 in a manner that can mirror our observations with the AAK1 and GAK siRNAs. First, we wanted to measure cytotoxicity of these compounds in U87MG cells. A range of three concentrations (1,5 and 10μM) of Aza and Erl, along with 0.1% DMSO as a control, were added to U87MG cells for 24 hours and cytotoxicity was determined via CellTiter-Glo. Aza and Erl were shown to be relatively non-toxic when compared to the DMSO control up to 10μM (Figure 5B). With toxicity levels determined, we next wanted to determine if Aza and Erl can inhibit TC-83 multiplication. U87MG cells treated for 2 hours with 10μM of Aza, 1μM Erl, and 0.1% DMSO as a control. The treated media was removed and the cells were incubated with TC-83 at an MOI:0.1 for 1 hour. The virus containing medium was removed, the drug containing medium was added back on for 18 hours. The supernatants were analyzed in Vero cells by plaque assay to quantify infectious viral titers. Results from the plaque assay experiments showed that both drugs exhibited inhibitory effects on TC-83 replication, with Aza treatment resulting in a 1-log decrease and Erl treatment resulting in a 2-log decrease in viral titers compared to the DMSO control (Figure 5A). Having shown treatment of cells with a non-toxic level of Aza and Erl results in a reduction in infectious viral titers, we measured the effect the inhibitors have on viral protein expression. Viral protein expression was determined by Western blot analysis on whole cell extracts from infected cells at an MOI:0.1 that were pretreated with Aza or Erl

as previously described. As controls, we used cells that were treated with DMSO, Aza, and Erl, but were not infected with TC-83, and DMSO cells that were infected. (Figure 5C). Three independent infections were set-up and whole cell extracts were analyzed at 18hpi, with levels of VEEV capsid and GP being normalized to β-actin. Treatment with Aza resulted in a decrease in the presence of capsid protein, with minimal change in glycoprotein expression, when compared to the infected DMSO control. Treatment with Erl yielded a dramatic increase in the intracellular levels of both capsid and glycoprotein. This was an interesting observation that is in contrast with our observation made with siRNAs (Figure 3). We reason that this discrepancy may reflect additional off target effects of the small molecule that may impact different arms of the secretory pathway and hence prevent viral assembly, without necessarily inhibiting viral gene expression from the subgenomic promoter. Together this shows that Aza decreases both viral protein expression and infectious titers, while treatment with Erl diminishes viral titers, but results in an accumulation of both viral proteins.

To determine the overall effectiveness and safety of treating U87MG cells with Aza and Erl, we next wanted to determine the cytotoxic concentration (CC_{50}) and effective concentration (EC_{50}). The CC_{50} is the concentration of drug at which 50% of cells are killed and the EC_{50} is the concentration at which 50% of the virus is killed. These two values are used to determine the selectivity index (SI) of candidate drugs (CC_{50}/EC_{50}) and potential for further development as a therapeutic. A high SI shows that a drug has strong antiviral properties at a concentration that will not harm the host, which is a desirable feature. The

CC_{50} values of both drugs were first determined to determine their overall cytotoxicity. U87MG cells seeded in a 96-well plate were incubated for 24 hours with varying concentrations of the inhibitors (1-100μM for Erl and 1-275μM for Aza) and 0.1% DMSO as a control, and cytotoxicity was measured using CellTiter-Glo assay. The CC_{50} for Aza was determined to be 269.1μM (Figure 6A) and 85.1μM for Erl (Figure 6C). With cytotoxicity levels determined, the next course of action was to ascertain the EC_{50} values. U87MG cells were seeded in 96-well plate and the following day pretreated for 2 hours with a range of nontoxic concentrations of Aza and Erl (0.01-10μM for Erl and 1-100μM for Aza) and DMSO as a control. Treated media was removed and the cells were incubated with TC-83 at an MOI:0.1 for 1 hour, followed by the removal of the viral media and the readdition of the treated media. The supernatants were collected after 18hpi and subsequently analyzed by plaque assay as previously described. Plaque analysis revealed that Aza has an EC_{50} of 7.5μM (Figure 6B) and Erl has an EC_{50} of 0.053μM (Figure 6D). The selectivity index (SI) was calculated (CC_{50}/EC_{50}) for both compounds and the SI's were determined to be 35 and 1605 for Aza and Erl respectively. These data demonstrate that Aza and Erl exhibit inhibitory effects on VEEV and does so at levels well below cytotoxic levels.

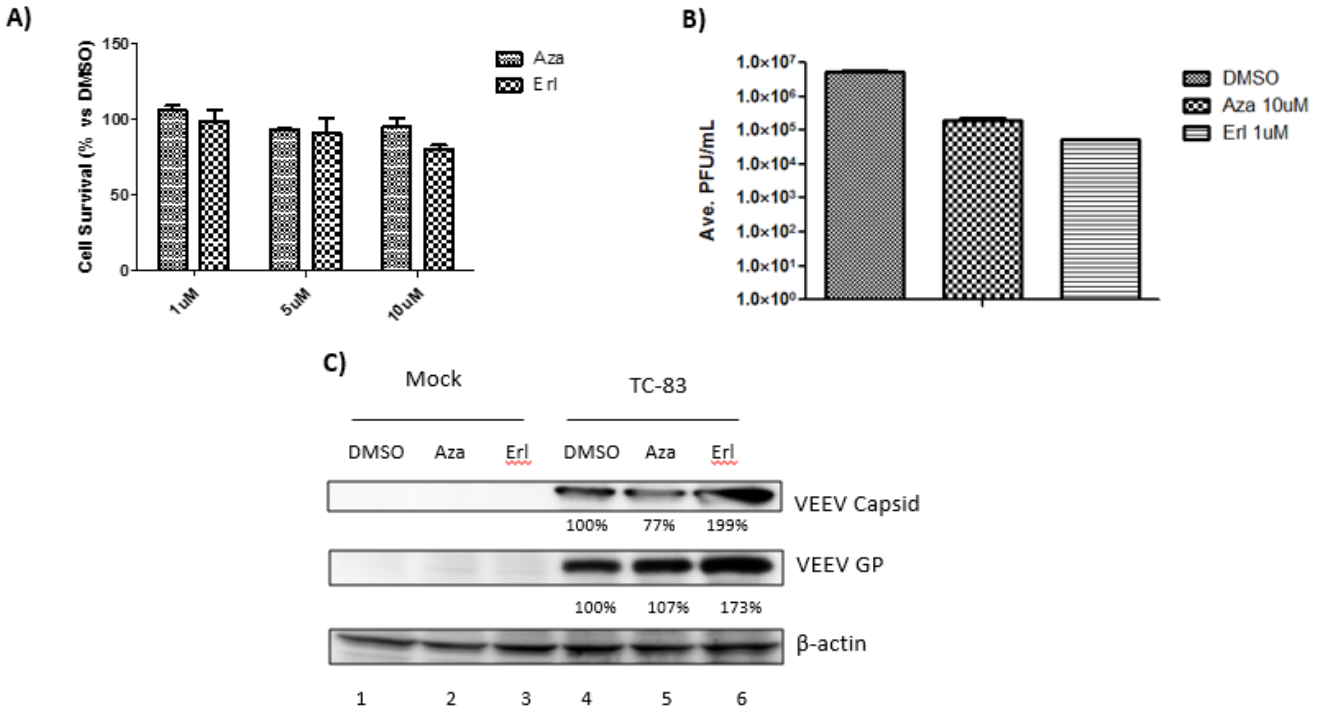

Figure 5. The kinase inhibitors Azaindole and Erlotinib inhibit VEEV replication and alter viral protein expression. U87MG cells were seeded into a 96-well plate at a concentration of 10,000 cells/well. After 24 hours, the cells were treated 0.1% DMSO, Aza, and Erl for 2 hours, infected with TC-83, and incubated for 18 hours. Supernatants were diluted and added to VERO cells for 48 hours, fixed, and stained for plaque analysis (A). Three concentrations of Aza and Erl were added to U87MG cells for 24 hours and cell viability was measured using CellTiter-Glo assay and compared to cells treated with 0.1% DMSO (B). Whole cell extracts of uninfected and infected cells treated with DMSO, Aza, and Erl were probed for VEEV capsid and glycoprotein and analyzed by Western blot with β-actin used as the standard (C).

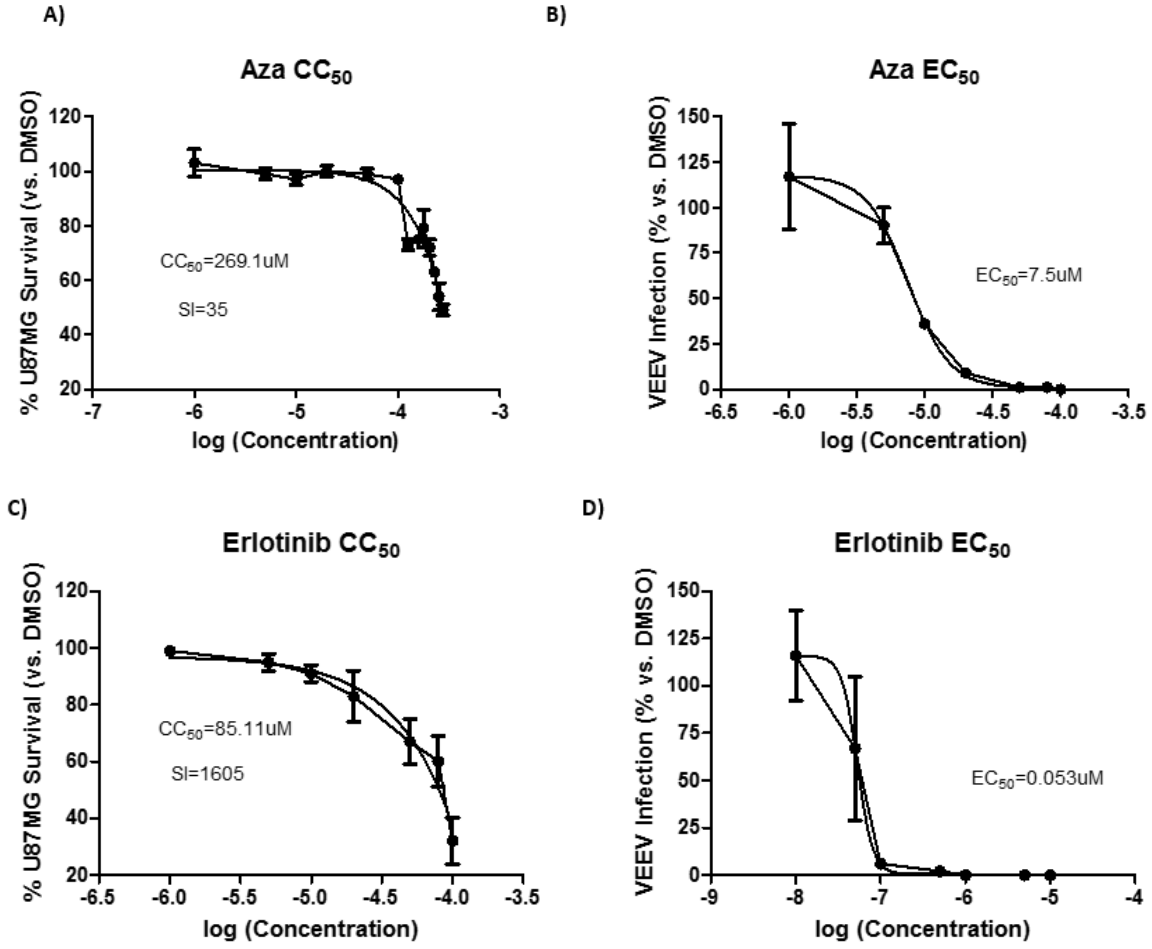

Figure 6. Cytotoxic concentration and effective concentration for Azaindole and Erlotinib. CC_{50} values were determined by treating U87MG cells with 0.1% DMSO, Aza (1-275μM) (A) and Erl (1-100μM) (C) for 24 hours and cytotoxicity levels measured via CellTiter-Glo. EC_{50} values were determined by treating U87MG cells with 0.1% DMSO, Aza (1-100μM) and Erl (0.01-10μM) for 2 hours, infecting with TC-83 for 1 hour, and incubated for 18 hours. Supernatants were added to VERO cells for 48 hours and plaque formation was analyzed and compared to the DMSO control (B, D). Drug concentrations are shown in log form.

Aza and Erl Exhibit Inhibitory Potential Against an Established VEEV Infection

As VEEV can replicate quickly and to high titers, it would be beneficial to therapeutically treat patients after a potential exposure event. As all treatments have been given pre-exposure to VEEV for prior experiments, we next wanted to determine if Aza and Erl have inhibitory potential when introduced as a post exposure strategy. U87MG cells were seeded and infected at an MOI:0.1 for 1 hour with TC-83. 10μM of Aza and 1μM Erl were added to independent wells at sequential time points (-2, 0, 2, 4 and 6hpi), as well as DMSO for a control (Figure 7A). Supernatants were collected at 18hpi for determination of intracellular genomic load and extracellular infectious titers by RT-qPCR and plaque analyses. Plaque analysis (Figure 7B) reveals that there is at least a log decrease in plaque forming units across all time points for both inhibitors. Intracellular RNA levels (Figure 8A) measured via RT-qPCR show a log drop in viral RNA for Aza treated cells when compared to the DMSO control, and comparable levels between Erl and DMSO treated cells. Extracellular RNA levels (Figure 8B) for Aza were at the same levels or higher as the DMSO control at the -2, 0, and 2hpi time points. At the 4 and 6hpi time points, there was a reduction in viral RNA levels, ~1.5 logs lower than the DMSO treated cells. Erl treated cells were 2 logs lower than the DMSO levels at the -2, 0, and 2hpi time points, with levels increasing 1 log or less lower than the DMSO at 4 and 6hpi time points. The compiled data shows that Aza and Erl are capable to VEEV inhibition when there is an established infection and hence, can be utilized as post-exposure therapeutics.

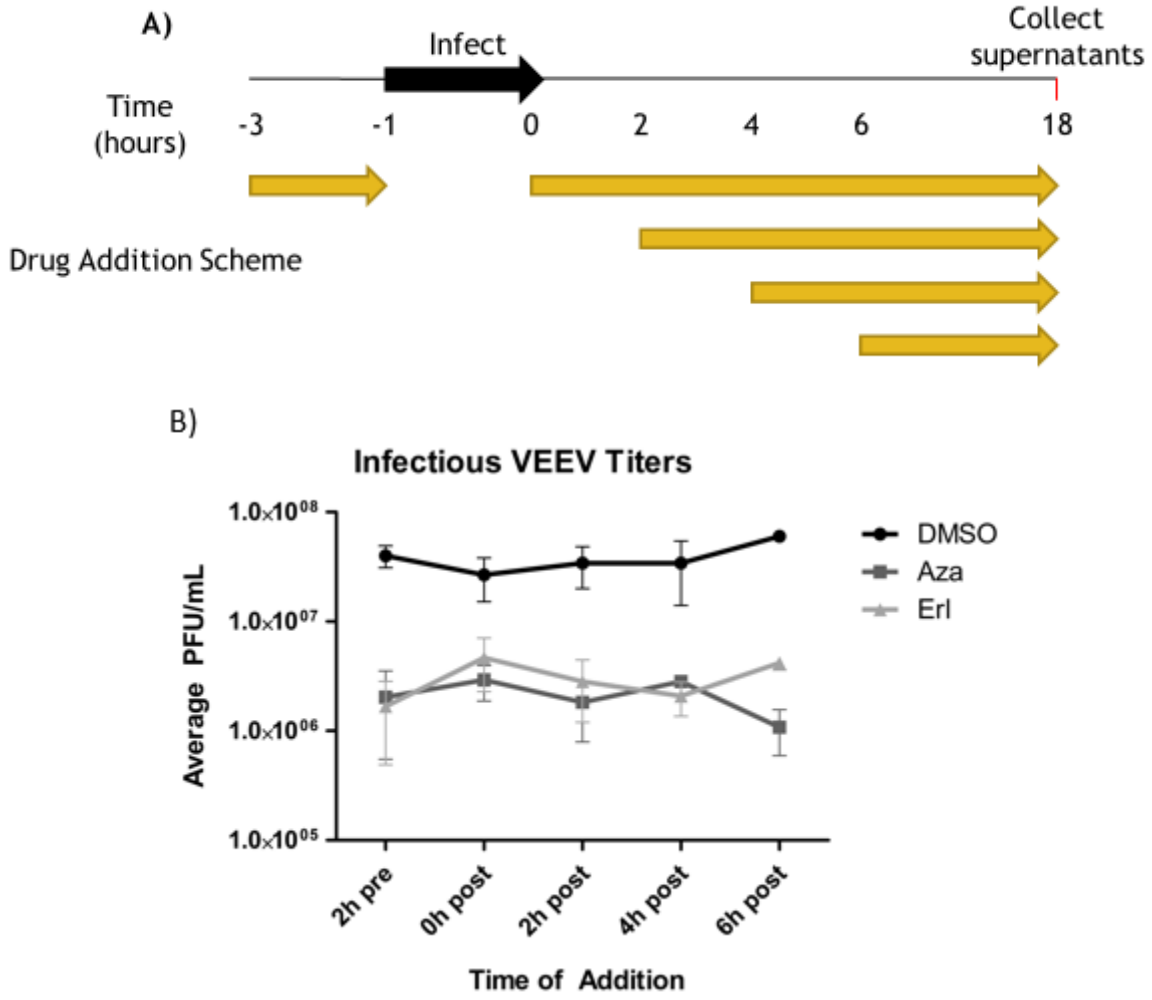

Figure 7. Levels of infectious VEEV titers when Azaindole and Erlotinib are used therapeutically. U87MG cells were seeded and infected with TC-83 at an MOI:0.1 for 1 hour. DMSO, Aza (10μM), and Erl (1μM) treated media was added to independent wells at time points of -2, 0, 2, 4, and 6hpi, and collected at 18hpi (A). Supernatants were diluted by factors of 10 and added to VERO cells for 48 hours and stained to detect plaques (B).

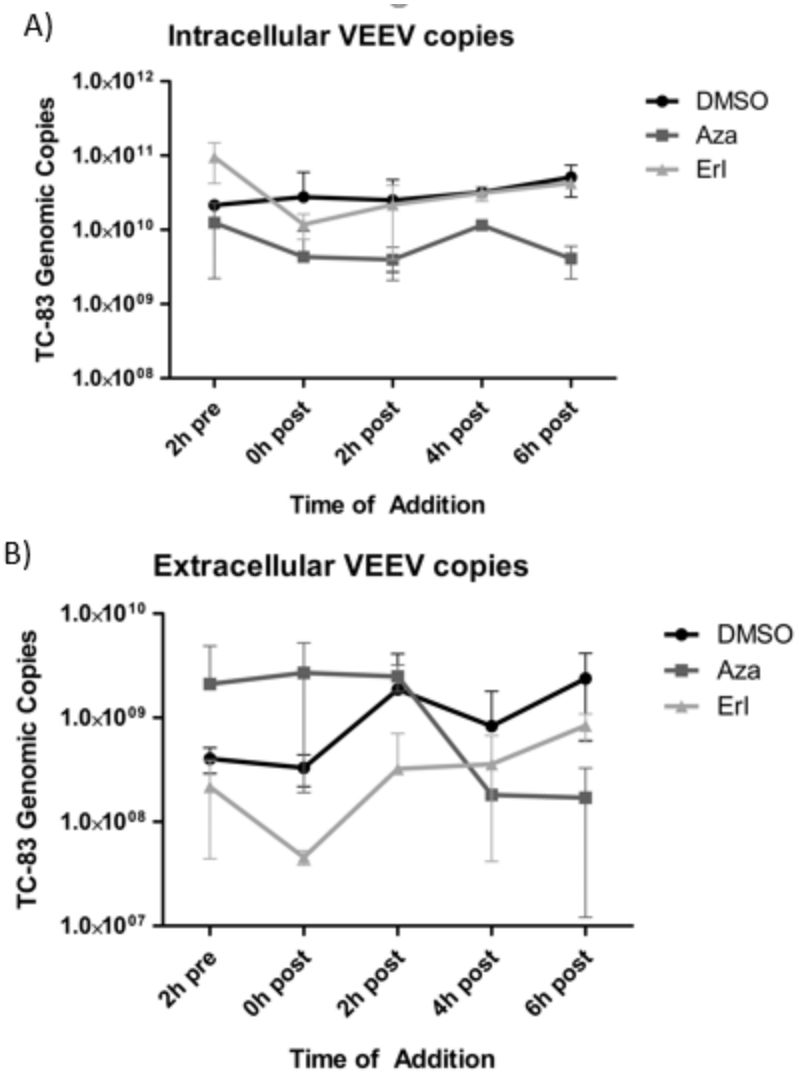

Figure 8. Intracellular and extracellular RNA levels of VEEV when Azaindole and Erlotinib are used therapeutically. U87MG cells were seeded and infected with TC-83 at an MOI:0.1 for 1 hour. DMSO, Aza (10μM), and Erl (1μM) treated media was added to independent wells at time points of -2, 0, 2, 4, and 6hpi, and collected at 18hpi. Intracellular (A) and extracellular (B) viral RNA was extracted and analyzed using RT-qPCR.

Mechanisms Involved in Viral Inhibition by Aza and Erl.

AP2 is required for clathrin mediated endocytosis. Based on the rationale that inhibition of AP2 mediated endocytosis will interfere with viral uptake, we anticipated that there will be an impact on viral entry when treated with Aza. We attempted to answer that question by confocal microscopy experiments to compare viral glycoprotein uptake in infected cells +/- Aza. U87MG cells were pre-treated for 2 hours with 10μM Aza and infected at an MOI:1 for 1h. The cells were fixed with 4% paraformaldehyde in PBS at 6hpi. This time point was chosen in order to try and visualize any potential impact in the early stage of infection, namely viral entry. Cells were permeabilized with Triton X-100, incubated with primary antibodies specific to AP2 and VEEV GP, incubated with Alexa-Fluor secondary antibodies, and mounted with DAPI Fluoromount G. Images were acquired using the 60X objective of a Nikon Eclipse TE2000 confocal microscope. All scale bars represent 20 microns. Images of uninfected cells show AP2 distributed throughout the cell. In contrast, the protein appeared to be more concentrated near the plasma membrane for those treated with Aza, even in the absence of infection that alludes to the impact that the drug as on AP2 distribution in cells. When infected but untreated, there appeared to be internal VEEV glycoprotein in the cells, in contrast to those that were treated with the inhibitor, where VEEV glycoprotein was observed to be more concentrated at the plasma membrane, however, treated cells show a colocalization of glycoprotein and AP2 at the plasma membrane (Figure 9). This data suggests that Aza prevents the trafficking of viral protein into the cell by inhibiting the activation of AP2.

We next wanted to determine if there is a similar viral trafficking hindrance occurring when cells are treated with Erl. AP1 is involved in the trafficking of clathrin coated vesicles at the trans-Golgi network. With the increase in viral protein levels noted in Erl treated cells (Figure 4), we hypothesize that Erl inhibits AP1 and the trafficking of viral proteins at a later point in infection, potentially involving the ER and/or golgi. To test our proposition, we infected U87MG cells as described for the Aza experiment, but pretreatment was done at 1μM with Erl and cells were fixed at 10hpi. This time point was chosen to allow for the VEEV infection to reach a time point in its life-cycle when it may be amenable to detect protein accumulation around the ER and/or Golgi regions. Cells were incubated with antibodies specific to either the RCSA1 Golgi marker, a transmembrane protein found predominately in the Golgi, the calnexin ER marker, a chaperone protein that associates with glycoproteins in the ER, or VEEV GP. All scale bars represent 20 microns. Confocal images show that treatment with Erl does not lead to a retention of VEEV glycoprotein within the Golgi (Figure 10). However, there was a modest accumulation of glycoprotein around the ER (Figure 11). The location where the bulk of viral proteins are being retained may potentially be located further along in the secretory pathway that may explain increased viral protein detection inside cells while there is a decrease in extracellular infectious viral load (Figure 4). The glycoproteins are processed through the secretory system after leaving the ER and Golgi and associate with the nucleocapsid at the cell membrane. It is possible that Erl has an inhibitory effect at this point between the Golgi and cell membrane, preventing the trafficking of the vesicle to the cell membrane. The data

shows that treatment with Erl leads to a modest retention of glycoprotein in the ER, but the location where the most retention is occurring has yet to be elucidated.

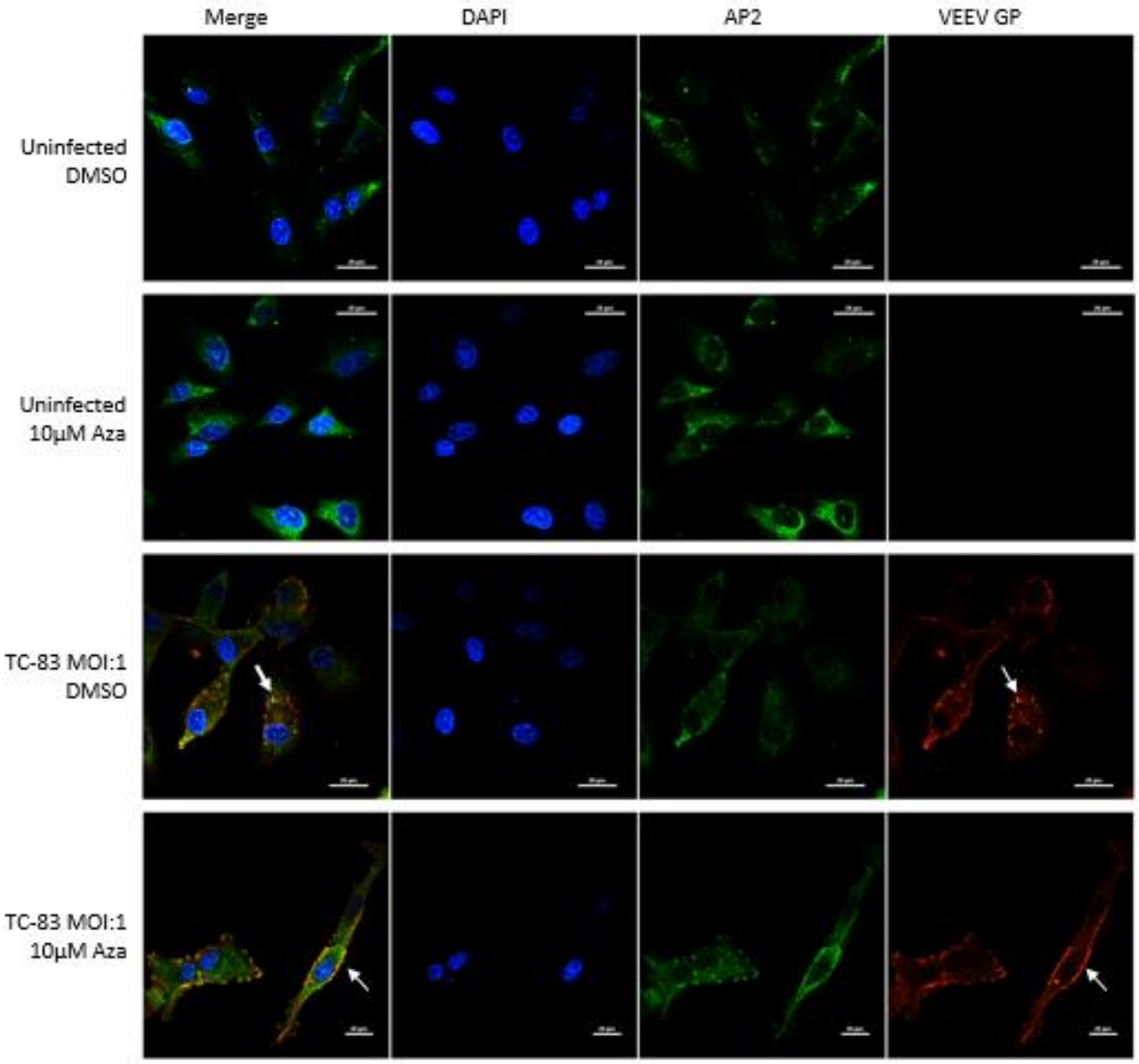

Figure 9. Treatment with Azaindole leads to an accumulation of VEEV GP at the cell membrane. Cells were pre-treated for 2 hours with 10μM Aza, infected at an MOI:1 for 1h, and fixed with 4% paraformaldehyde in PBS at 6hpi. Cells were permeabilized with Triton X-100, incubated with primary antibodies specific to AP2 and VEEV GP, incubated with Alexa-Fluor secondary antibodies (Alexa Flour 488 for green, 567 for red), and mounted with DAPI Fluoromount G. Images were taken using the 60X objective of a Nikon Eclipse TE2000 confocal microscope. All scale bars represent 20 microns. Arrows are used to show areas of viral protein accumulation.

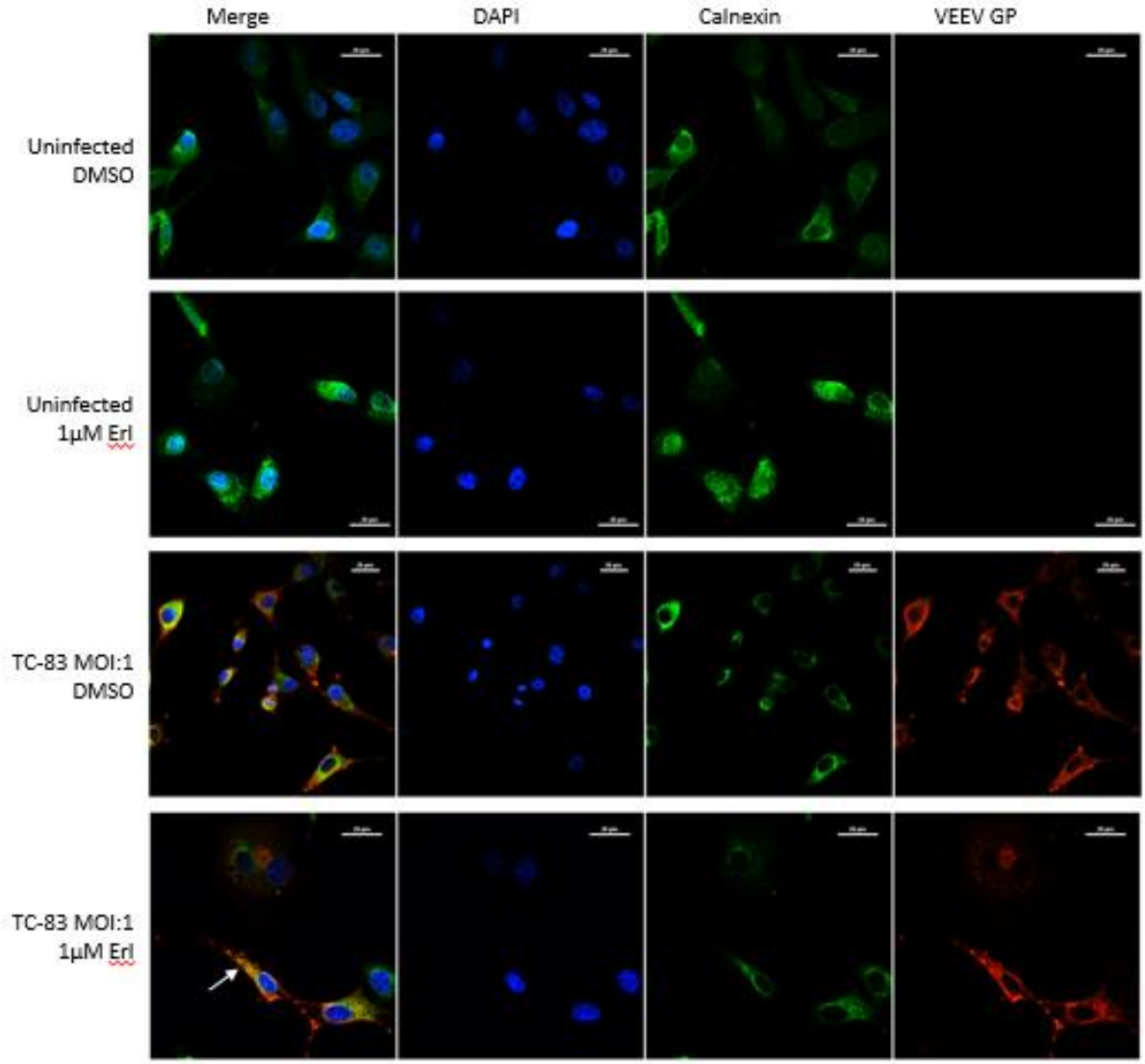

Figure 10. Treatment with Erltotinib leads to a modest accumulation of VEEV GP at the ER. U87MG cells were pre-treated for 2 hours with 1μM Erl, infected at an MOI:1 for 1h, and fixed with 4% paraformaldehyde at 10hpi. Cells were incubated with antibodies specific to the calnexin ER marker and VEEV GP. incubated with Alexa-Fluor secondary antibodies (Alexa Flour 488 for green, 567 for red), and mounted with DAPI Fluoromount G. Images were taken using the 60X objective of a Nikon Eclipse TE2000 confocal microscope. All scale bars represent 20 microns. Arrows are used to show areas of viral protein accumulation.

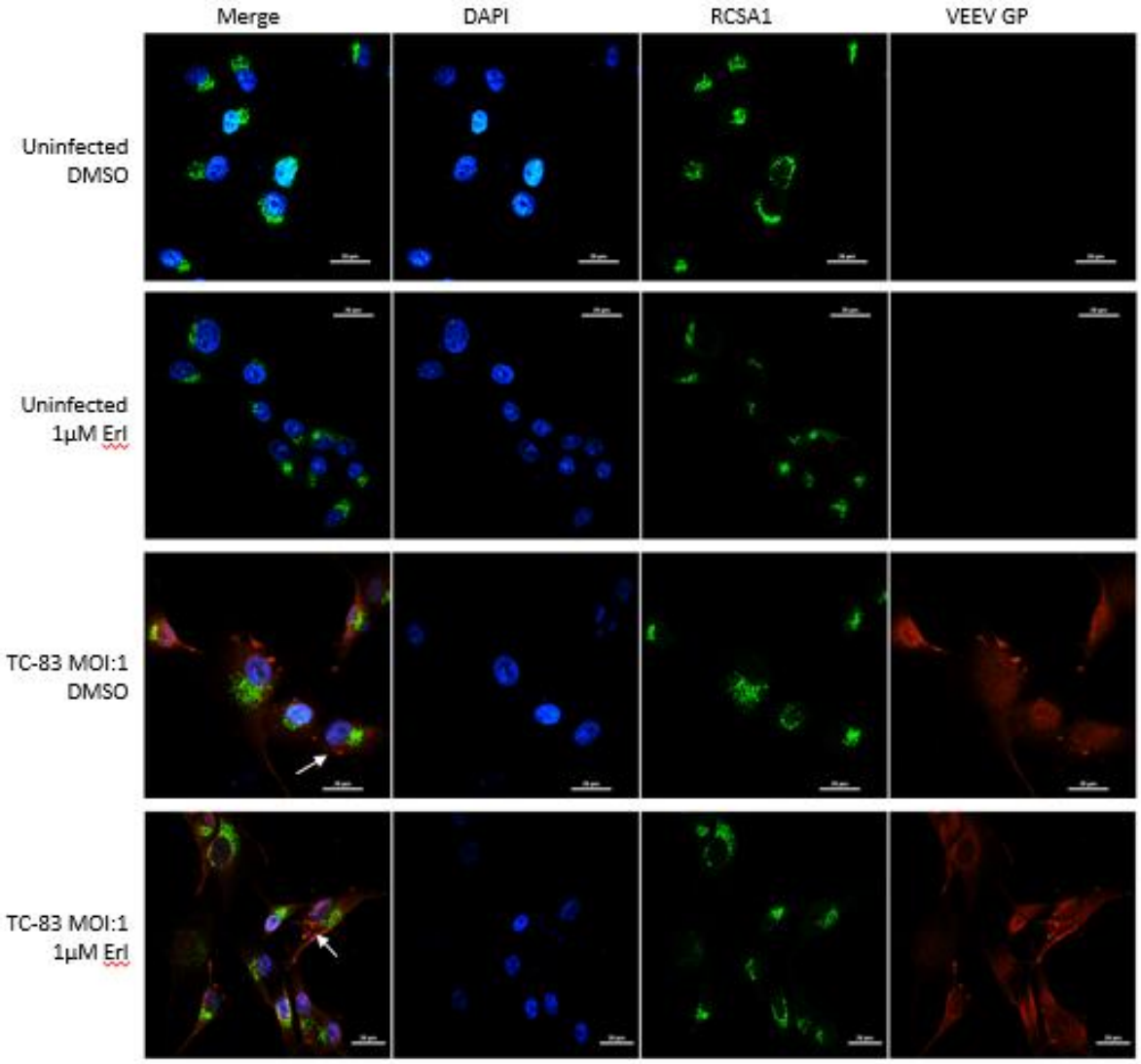

Figure 11. Treatment with Erlotinib does not lead to an accumulation of VEEV GP at the Golgi. U87MG cells were pre-treated for 2 hours with 1µM Erl, infected at an MOI:1 for 1h, and fixed with 4% paraformaldehyde at 10hpi. Cells were incubated with antibodies specific to the RCSA1 Golgi marker and VEEV GP, incubated with Alexa-Fluor secondary antibodies (Alexa Flour 488 for green, 567 for red), and mounted with DAPI Fluoromount G. Images were taken using the 60X objective of a Nikon Eclipse TE2000 confocal microscope. All scale bars represent 20 microns. Arrows are used to show areas of viral protein accumulation.

Future Work

As both Aza and Erl were shown to be effective against VEEV, we are currently exploring the synergistic effects of both drugs. While the lack of an additive effect observed when both AAK1 and GAK were silenced using siRNAs, it is possible that the small molecule inhibitors may not show the same result, as was evidenced in the differences between Aza/Erl and siRNA data. As well as this, we are looking to define the connection between AAK1/GAK inhibition on AP1/AP2 function. In order to define the active sites on AP1 and AP2 that are needed for the trafficking of viral proteins, we are using phosphorylation overexpression plasmids that contain mutations in the M1 or M2 subunits of AP1 and AP2. Having shown that mutations in this region effects trafficking in other viruses [24-26], we want to establish if these activation sites influence clathrin-mediated trafficking for VEEV.

CHAPTER 4: DISCUSSION

The capability to efficiently replicate to high titers and maintain infectivity when aerosolized, along with the current absence of a vaccine, make VEEV an important focus of research and development of novel strategies for therapeutic intervention. Targeting viral components as candidates for inhibition increases the risk for mutations within the virus and the development of drug resistance. However, targeting host proteins that have critical roles to play in the establishment of an infectious cycle circumvents the concern of viral resistance, as well as offers the potential for broad spectrum inhibition. Inhibition of clathrin-associated AP1 and AP2 by targeting the kinases that activate them, AAK1 and GAK, has been shown to have an antagonistic effect on HCV, DENV, and EBOV [23-25]. Given the role of clathrin-mediated endocytosis on viral infections in the case of enveloped viruses, we hypothesized that this pathway will be critical for the establishment of a productive VEEV infection. To that effect, in this effort we have addressed VEEV's dependency on clathrin-mediated endocytosis for entry and trafficking, and the effects of inhibition of AAK1 and GAK on VEEV's life cycle.

We first demonstrated that a knockdown of AAK1 and GAK using siRNAs results in both a decrease in viral titers and protein expression (Figure 4). Intracellular RNA levels

were significantly lowered for AAK1 knockdown, with a more modest reduction for GAK knockdown. Plaque forming units were dramatically decreased for both kinase knockdowns, however, no synergistic effect was observed when both were silenced. The absence of an additive effect when both kinases are silenced may be due to a maximum inhibition level being reached when entry is inhibited. At those concentrations, the siRNAs may be preventing each other from silencing more protein as they are in competition with each other for the RNA induced silencing complex. This would prevent the two siRNAs from building upon each other. VEEV capsid levels in the cell was greatly reduced when AAK1 was silenced, along with a fair reduction in VEEV GP. This larger drop in capsid levels could be a result of the early inhibition of viral entry that silencing of AAK1 would have. The nucleocapsid is released after viral entry and fusion with the endosome. AAK1 activates AP2, which is involved in the vesicle formation at the cell membrane. Inhibition of AP2 may diminish the amount of capsid that is entering the cell, as this is released after the fusion of the viral envelope with the endosome. A similar result was observed with GAK knockdown, but with the levels of GP being more diminished than capsid. VEEV glycoprotein goes through the ER and Golgi for processing. GAK activates AP1, which is involved in trafficking around the Golgi, so this inhibition can account for the larger reduction in glycoprotein. However, these data does not point to a decrease in gene expression from the subgenomic promoter.

Our siRNA experiments suggested a strong dependence of VEEV on AAK1 and GAK activity which led us to investigate if small molecule inhibits of these kinases could be effectively developed as anti-alphavirus therapeutic candidates, to that effect, we

investigated if two small molecules, Aza and Erl, with known inhibitory effect against AAK1 and GAK, were capable of controlling VEEV infection in cell culture. Our quantification of CC_{50} and EC_{50} values for both drugs shows high selective indexes for both (Figure 6), showing that they can be effective at levels that won't harm the host. Analysis of viral protein levels showed that there was a modest drop in VEEV capsid, with no net change in glycoprotein levels when cells were treated with Aza. Interestingly, treatment with Erl lead to a dramatic increase in both viral proteins. Comparing the protein levels to those found in the siRNA treated cells, there were some notable differences. Both Aza and AAK1 treated cells had a reduction in capsid, though not as drastic in the Aza treated cells, and no reduction in GP for Aza whereas there was some noted in AAK1 treated cells. GAK siRNA treated cells had a reduction in both proteins, while Erl treated cells had an increase. These differences may be a result of the targeting of the siRNAs when compared to the small molecule inhibitors. siRNAs will bind only to one specific target, so those cells show what inhibition of just those proteins will have on viral replication. Small molecule inhibitors don't have the same specificity and may influence other targets. Erlotinib is known to also target the epidermal growth factor, and Aza is also a known inhibitor of other kinases, such as Abl and Src kinases, in the treatment of cancer. It is possible that the influence of other kinases may be resulting in the differences that that are seen between the siRNAs and small molecule inhibitors. We examined the potential for these inhibitors to be used therapeutically (Figure 7 and Figure 8). Time of addition experiments exhibited that treatment with Aza and Erl both lead to a decrease in viral infectious titers at both pre-and post-exposure times. Intracellular RNA levels were

reduced across all time points for Aza treated cells, and interestingly, a spike initially in extracellular RNA, followed by a decrease. For Erl, extracellular levels were reduced across all time points and no changes in intracellular levels compared to the control. This reduction shows that both Aza and Erl are efficacious against VEEV when used therapeutically.

Having elucidated the potential for Aza and Erl to inhibit VEEV, we next examined the points in the viral lifecycle that these drugs are impeding (Figure 9-11). Confocal imagery showed that treatment with Aza leads to an accumulation of AP2 and viral protein at the plasma membrane. The combined data show that entry into the cell is reduced because of AP2 being retained at the plasma membrane. AP2 aids in clathrin-mediated endocytosis at the cell membrane, the entry mechanism used by VEEV. Treatment with Aza is inhibiting the AP2 from associating with the endosome and allowing it to mature, hindering entry of VEEV into the cell. When treated with Erl, there is a retention of VEEV glycoprotein at the ER but not at the Golgi. Erl appears to block the trafficking of the viral proteins to the plasma membrane for budding, possibly through inhibition of AP1. The drastic increase in viral protein levels and drop in extracellular copies would support this prediction. What remains to be determined is where much of this obstruction is occurring. With no retention at the Golgi and modest retention at the ER, most of the inhibition may be occurring between the plasma membrane and the Golgi, in clathrin-associated vesicles of the secretory pathway.

We are further exploring the connection between AAK1/GAK inhibition on AP1/AP2 function. Using phosphorylation overexpression mutant plasmids, we are trying to determine what the active site is on AP1 and AP2 that traffics the viral proteins. Prior work using AP2 plasmids with a T156A mutation in the M1 subunit resulted in inhibition of HCV, DENV, and EBOV, and a T144A mutation in the M1 subunit of AP1 had a similar effect in HCV (24-26). With this inhibition occurring in multiple viruses that utilize the same proteins, it is plausible that activation of these sites by AAK1 and GAK are the mechanism behind clathrin-mediated VEEV trafficking. Also, we are exploring the synergistic effects of Aza and Erl. With both showing favorable inhibition effects, it is worth elucidating if there is an additive effect when they are used in combination.

Taken together, we believe our data supports our hypothesis that VEEV is susceptible to inhibition of AAK1 and GAK by small molecule inhibitors. We showed that inhibition of the kinases with Aza and Erl reduces the amount of infectious viral titers and VEEV genomic copies when used prophylactically and against established VEEV infections. An effect on viral protein production was observed for both inhibitors, a decrease with Aza treatment and an increase with Erl treatment. Aza may have inhibited the entry of virus into the host cell, and Erl caused an accumulation of viral proteins, suggestive of inhibition of the capability of the virus to exit.

REFERENCES

1. Jose, J., Snyder, J. E., & Kuhn, R. J. (2009). A structural and functional perspective of alphavirus replication and assembly. *Future Microbiology*, *4*, 837–856. http://doi.org/10.2217/fmb.09.59
2. Foy, N. J., Akhrymuk, M., Akhrymuk, I., Atasheva, S., Bopda-Waffo, A., Frolov, I., & Frolova, E. I. (2013). Hypervariable Domains of nsP3 Proteins of New World and Old World Alphaviruses Mediate Formation of Distinct, Virus-Specific Protein Complexes. *Journal of Virology*, *87*(4), 1997–2010. http://doi.org/10.1128/JVI.02853-12
3. Go, Y. Y., Balasuriya, U. B., & Lee, C. K. (2014). Zoonotic encephalitides caused by arboviruses: transmission and epidemiology of alphaviruses and flaviviruses. *Clinical and experimental vaccine research*, *3*(1), 58-77. https://doi.org/10.7774/cevr.2014.3.1.58
4. Brooke, C. B., Schäfer, A., Matsushima, G. K., White, L. J., & Johnston, R. E. (2012). Early activation of the host complement system is required to restrict central nervous system invasion and limit neuropathology during Venezuelan equine encephalitis virus infection. *The Journal of General Virology*, *93*(Pt 4), 797–806. http://doi.org/10.1099/vir.0.038281-0

5. Aguilar, P. V., Estrada-Franco, J. G., Navarro-Lopez, R., Ferro, C., Haddow, A. D., & Weaver, S. C. (2011). Endemic Venezuelan equine encephalitis in the Americas: hidden under the dengue umbrella. *Future Virology*, *6*(6), 721–740. http://doi.org/10.2217/FVL.11.5

6. Paessler, S., & Weaver, S. C. (2009). Vaccines for Venezuelan equine encephalitis. *Vaccine*, *27S4*, D80–D85. http://doi.org/10.1016/j.vaccine.2009.07.095

7. Weaver, S. C., Ferro, C., Barrera, R., Boshell, J., & Navarro, J. C. (2004). Venezuelan equine encephalitis. *Annual Reviews in Entomology*, *49*(1), 141-174. https://doi.org/10.1146/annurev.ento.49.061802.123422

8. Amaya, M., Voss, K., Sampey, G., Senina, S., de la Fuente, C., Mueller, C., Calvert, V., Kehn-Hall, K., Carpenter, C., Kashanchi, F., Bailey, C., Mogelsvang, S., Petricoin, E., & Narayanan, A. (2014). The Role of IKKβ in Venezuelan Equine Encephalitis Virus Infection. *PLoS ONE*, *9*(2), e86745. http://doi.org/10.1371/journal.pone.0086745

9. Amaya, M., Brooks-Faulconer, T., Lark, T., Keck, F., Bailey, C., Raman, V., & Narayanan, A. (2016). Venezuelan equine encephalitis virus non-structural protein 3 (nsP3) interacts with RNA helicases DDX1 and DDX3 in infected cells. *Antiviral research*, *131*, 49-60. https://doi.org/10.1016/j.antiviral.2016.04.008

10. Paredes, A., Alwell-Warda, K., Weaver, S. C., Chiu, W., & Watowich, S. J. (2001). Venezuelan equine encephalomyelitis virus structure and its divergence from Old World alphaviruses. *Journal of virology*, *75*(19), 9532-9537. https://doi.org/10.1128/jvi.75.19.9532-9537.2001

11. Strauss, J. H., & Strauss, E. G. (1994). The alphaviruses: gene expression, replication, and evolution. *Microbiological Reviews*, *58*(3), 491–562.
12. Beitzel, B. F., Bakken, R. R., Smith, J. M., & Schmaljohn, C. S. (2010). High-resolution functional mapping of the venezuelan equine encephalitis virus genome by insertional mutagenesis and massively parallel sequencing. *PLoS pathogens*, *6*(10), e1001146. https://doi.org/10.1371/journal.ppat.1001146
13. Voss, K., Amaya, M., Mueller, C., Roberts, B., Kehn-Hall, K., Bailey, C., Petricoin, E., & Narayanan, A. (2014). Inhibition of host extracellular signal-regulated kinase (ERK) activation decreases New World alphavirus multiplication in infected cells. *Virology*, *468*, 490-503. http://doi.10.1016/j.virol.2014.09.005
14. Gridina, M. M., Protopopova, E. V., Kachko, A. V., Ivanova, A. V., Bondarenko, E. I., & Loktev, V. B. (2007). Cellular laminin-binding protein and Venezuelan equine encephalomyelitis virus replication in Vero, 293 and 9S2 cells. *Cell and Tissue Biology*, *1*(6), 491-496.
15. Kielian, M., Chanel-Vos, C., & Liao, M. (2010). Alphavirus Entry and Membrane Fusion. *Viruses*, *2*(4), 796–825. http://doi.org/10.3390/v2040796
16. Leung, J. Y.-S., Ng, M. M.-L., & Chu, J. J. H. (2011). Replication of Alphaviruses: A Review on the Entry Process of Alphaviruses into Cells. *Advances in Virology*, *2011*, 249640. http://doi.org/10.1155/2011/249640
17. Kirchhausen, T., Owen, D., & Harrison, S. C. (2014). Molecular Structure, Function, and Dynamics of Clathrin-Mediated Membrane Traffic. *Cold Spring Harbor Perspectives in Biology*, *6*(5), a016725. http://doi.org/10.1101/cshperspect.a016725

18. Royle, S. J. (2006). The cellular functions of clathrin. *Cellular and Molecular Life Sciences : CMLS*, *63*(16), 1823–1832. http://doi.org/10.1007/s00018-005-5587-0

19. Bonnemaison, M. L., Eipper, B. A., & Mains, R. E. (2013). Role of Adaptor Proteins in Secretory Granule Biogenesis and Maturation. *Frontiers in Endocrinology*, *4*, 101. http://doi.org/10.3389/fendo.2013.00101

20. Motley, A. M., Berg, N., Taylor, M. J., Sahlender, D. A., Hirst, J., Owen, D. J., & Robinson, M. S. (2006). Functional Analysis of AP-2 α and μ2 Subunits. *Molecular Biology of the Cell*, *17*(12), 5298–5308. http://doi.org/10.1091/mbc.E06-05-0452

21. Zhang, C. X., Engqvist-Goldstein, Å. E., Carreno, S., Owen, D. J., Smythe, E., & Drubin, D. G. (2005). Multiple Roles for Cyclin G-Associated Kinase in Clathrin-Mediated Sorting Events. *Traffic*, *6*(12), 1103-1113. doi:10.1111/j.1600-0854.2005.00346.x

22. Lee, D. W., Zhao, X., Zhang, F., Eisenberg, E., & Greene, L. E. (2005). Depletion of GAK/auxilin 2 inhibits receptor-mediated endocytosis and recruitment of both clathrin and clathrin adaptors. *Journal of Cell Science*, *118*(18), 4311-4321. doi: 10.1242/jcs.02548

23. Ricotta, D., Conner, S. D., Schmid, S. L., von Figura, K., & Höning, S. (2002). Phosphorylation of the AP2 μ subunit by AAK1 mediates high affinity binding to membrane protein sorting signals. *The Journal of cell biology*, *156*(5), 791-795. doi: 10.1083/jcb.200111068

24. Neveu, G., Ziv-Av, A., Barouch-Bentov, R., Berkerman, E., Mulholland, J., & Einav, S. (2015). AP-2-Associated Protein Kinase 1 and Cyclin G-Associated

Kinase Regulate Hepatitis C Virus Entry and Are Potential Drug Targets. *Journal of Virology*, *89*(8), 4387–4404. http://doi.org/10.1128/JVI.02705-14

25. Bekerman, E., Neveu, G., Shulla, A., Brannan, J., Pu, S. Y., Wang, S., Xiao, F., Barouch-Bentov, R., Bakken, R.R., Mateo, R., Govero, J., Nagamine, C.M., Diamond, M.S., De Jonghe, S., Herdewijn, P., Dye, J.M., Randall, G., & Einav, S. (2017). Anticancer kinase inhibitors impair intracellular viral trafficking and exert broad-spectrum antiviral effects. *The Journal of Clinical Investigation*, *127*(4), 1338-1352. https://doi.org/10.1172/JCI89857
26. Neveu, G., Barouch-Bentov, R., Ziv-Av, A., Gerber, D., Jacob, Y., & Einav, S. (2012). Identification and Targeting of an Interaction between a Tyrosine Motif within Hepatitis C Virus Core Protein and AP2M1 Essential for Viral Assembly. *PLoS Pathogens*, *8*(8), e1002845. http://doi.org/10.1371/journal.ppat.10028
27. Smit, M. A., Maddalo, G., Greig, K., Raaijmakers, L. M., Possik, P. A., van Breukelen, B., Cappadona, S., Heck, A.J.R., Altelaar, A.F.M, Peeper, D. S. (2014). ROCK1 is a potential combinatorial drug target for BRAF mutant melanoma. *Molecular Systems Biology*, *10*(12), 772. http://doi.org/10.15252/msb.20145450

BIOGRAPHY

Tyler Lark was born and raised in Pennsylvania. He graduated from Lycoming College in 2010 with B.S. in Biology: Anatomy & Physiology. He began working for Quest Diagnostics in 2010 as a Cytogenetic Technologist. He will be receiving his Masters of Science in Biology from George Mason University in the Fall of 2017.